CRYSTAL GROWTH & DESIGN

Article

pubs.acs.org/crystal

Structural Conversion and Magnetic Studies of Low-Dimensional $Ln^{III}/Mo^{V/IV}(CN)_8$ (Ln = Gd−Lu) Systems: From Helical Chain to Trinuclear Cluster

Hu Zhou,[†] Qi Chen,[‡] Hong-Bo Zhou,[§] Xiao-Zhen Yang,[†] You Song,*[,⊥] and Ai-Hua Yuan*[,‡]

[†]School of Material Science and Engineering and [‡]School of Environmental and Chemical Engineering, Jiangsu University of Science and Technology, Zhenjiang 212003, P. R. China

[§]School of Chemistry and Chemical Engineering, Jiangsu University, Zhenjiang 212013, P. R. China

[⊥]State Key Laboratory of Coordination Chemistry, Nanjing National Laboratory of Microstructures, School of Chemistry and Chemical Engineering, Nanjing University, Nanjing 210093, P. R. China

Supporting Information

ABSTRACT: The slow diffusion reaction of octacyanometallate $[Mo^{V}(CN)_8]^{3-}$, lanthanide ions (Gd−Lu), and 1,10-phenanthroline (phen) in CH_3CN/H_2O has yielded eight isostructural one-dimensional chains, $[Ln^{III}(phen)_2(H_2O)Mo^{V}(CN)_8]_2[(n\text{-}C_4H_9)_4N](NO_3)\cdot 2CH_3CN\cdot 4H_2O$ (Ln = Gd(**1**), Tb(**2**), Dy(**3**), Ho(**4**), Er(**5**), Tm(**6**), Yb(**7**), Lu(**8**)), in which $[Ln^{III}(phen)_2(H_2O)]^{3+}$ and $[Mo^{V}(CN)_8]^{3-}$ units are linked alternatively through cyanide groups, generating left- and right-handed helices. Interestingly, **1**−**8** undergo a resolvation−recrystallization process upon prolonging the diffusion-reaction time, together with the valence change from V to IV of Mo center and structural dimensionalities switching from helical chains to trinuclear clusters, $(Hphen)_{2.5}[Ln^{III}_{0.5}(phen)(H_2O)][Mo^{IV}(CN)_8]\cdot 1.5CH_3CN$ (Ln = Gd(**9**), Tb(**10**), Dy(**11**), Ho(**12**), Er(**13**), Tm(**14**), Yb(**15**), Lu(**16**)). Magnetic studies of **1**−**16** revealed the typical effects induced by single-ion magnetic anisotropy and/or the population of low-lying excited states, and **11** and **13** showed extraordinary field-induced slow magnetic relaxations.

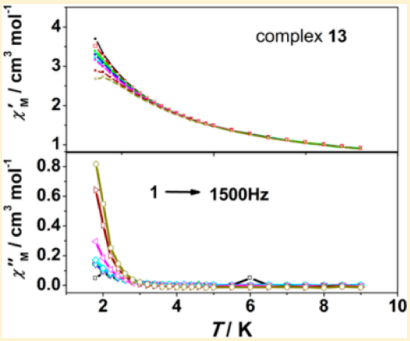

INTRODUCTION

In recent decades, considerable efforts have been devoted to the design and construction of molecule-based magnets owing to their functionalities and potential applications.[1] To attain such type of materials it would be highly desirable to elaborate a system with strong magnetic coupling and structural predictabilities. One of the promising systems is the cyanide-bridged assembly because cyanide groups can serve as a short-range mediator between spin carriers, and their magnetic nature is mainly dependent on magnetic orbitals of metal constituents. These materials have shown a remarkable diversity of magnetic properties such as high Curie temperatures,[2−4] ferroelectricity-ferromagnetism,[5,6] humidity-sensitive magnetism,[7−9] metamagnetism,[10] photoinduced magnetization,[11−15] etc.

In the case of discrete molecules or one-dimensional (1D) chains, cyanide-bridged single-molecule magnets (SMMs) or single-chain magnets (SCMs) have received special attention due to their peculiar slow magnetic relaxations and potential applications in information recording and storage devices. Particular examples of discrete molecules with large-spin group states include the $\{M^{II}_9M'^{V}_6(CN)_{48}(solv)_{24}\}$ (M = Mn(II), Co(II), Ni(II), Fe(II); M′ = Mo, W, Re; solv = MeOH, EtOH, H_2O) clusters derived from $[M'^{V}(CN)_8]^{3-}$ precursors, some of which have exhibited fascinating SMMs behaviors,[16−23] while SCMs characteristics were also observed in 1D chains.[24−28] To fabricate low-dimensional cyanide-based systems, the general synthetic methodology is to employ the aromatic chelated ligands to control the number and spatial arrangement of coordination positions available on the cation for CN-bridging, hence restricting the structural evolution toward higher dimensionalities. This recognition has inspired our group to fabricate low-dimensional hexa- and octacyanometallate-based assemblies.[29−32] For instance, the first cyanide-bridged lanthanide helical chains $\{Ln^{III}M^{V}\}$ (Ln = Pr, Sm, Eu; M = Mo, W) were synthesized by using bidentate 1,10-phenanthroline (phen) or 3,4,7,8-tetramethyl-1,10-phenanthroline (tmphen) as chelated and blocking ligands, where antiferromagnetic coupling interactions were observed between Ln(III) and M(V) centers.[31]

As is well-known, the magnetic susceptibilities of lanthanide system with strong spin−orbit coupling are obviously influenced by the thermal population of sublevels in the ground-state multiple in the ligand field. The magnetic characteristics can be altered systematically by varying lanthanide ions while maintaining identical geometries and ligand compositions.[33,34] On the basis of these considerations

Received: December 17, 2015
Revised: February 12, 2016

DOI: 10.1021/acs.cgd.5b01782
Cryst. Growth Des. XXXX, XXX, XXX−XXX

Table 1. Crystallographic Data and Structural Refinement for 1-8

	1	2	3	4	5	6	7	8
formula	$C_{84}H_{86}Gd_2Mo_2N_{28}O_9$	$C_{84}H_{86}Tb_2Mo_2N_{28}O_9$	$C_{84}H_{86}Dy_2Mo_2N_{28}O_9$	$C_{84}H_{86}Ho_2Mo_2N_{28}O_9$	$C_{84}H_{86}Er_2Mo_2N_{28}O_9$	$C_{84}H_{86}Tm_2Mo_2N_{28}O_9$	$C_{84}H_{86}Yb_2Mo_2N_{28}O_9$	$C_{84}H_{86}Lu_2Mo_2N_{28}O_9$
M_r	2138.19	2141.53	2148.69	2153.55	2158.21	2161.55	2169.77	2173.63
crystal system	tetragonal	tetragonal	tetragonal	tetragonal	tetragonal	tetragonal	tetragonal	tetragonal
space group	$I4_1/acd$	$I4_1/acd$	$I4_1/acd$	$I4_1/acd$	$I4_1/acd$	$I4_1/acd$	$I4_1/acd$	$I4_1/acd$
a (Å)	36.5091(13)	36.155(2)	36.3198(15)	36.5237(17)	36.2210(17)	37.0184(15)	36.2487(16)	36.1477(18)
b (Å)	36.5091(13)	36.155(2)	36.3198(15)	36.5237(17)	36.2210(17)	37.0184(15)	36.2487(16)	36.1477(18)
c (Å)	16.7776(11)	16.5928(10)	16.8296(16)	15.9657(11)	16.7841(8)	15.0002(12)	16.7213(15)	16.6610(13)
α (deg)	90.00	90.00	90.00	90.00	90.00	90.00	90.00	90.00
β (deg)	90.00	90.00	90.00	90.00	90.00	90.00	90.00	90.00
γ (deg)	90.00	90.00	90.00	90.00	90.00	90.00	90.00	90.00
V/Å^3	22363(2)	21690(2)	22200(2)	21298(2)	22020.1(18)	20556(2)	21971(2)	21770(2)
Z	8	8	8	8	8	8	8	8
ρ_c (g cm^{-3})	1.270	1.312	1.286	1.343	1.302	1.397	1.312	1.326
μ (mm^{-1})	1.447	1.573	1.609	1.760	1.790	2.011	1.968	2.082
total, unique	83065, 5502	80058, 5340	82454, 5475	77853, 5241	81915, 5410	75248, 5074	83424, 5413	80470, 5354
observed $[I > 2\sigma(I)]$	3480	3296	3207	3345	3327	3604	3135	3320
GOF on F^2	1.032	1.089	1.013	1.044	1.015	1.070	1.067	1.071
R_1, ωR_2 $[I > 2\sigma(I)]$	0.0451, 0.1272	0.0460, 0.1070	0.0503, 0.1356	0.0540, 0.1276	0.0578, 0.1634	0.0433, 0.1069	0.0541, 0.1411	0.0588, 0.1588
R_1, ωR_2 (all data)	0.0537, 0.1281	0.0509, 0.1074	0.0629, 0.1367	0.0596, 0.1281	0.0682, 0.1644	0.0518, 0.1079	0.0708, 0.1424	0.0690, 0.1597
CCDC number	1421793	1421794	1421795	1421796	1421797	1421798	1421799	1421800

DOI: 10.1021/acs.cgd.5b01782
Cryst. Growth Des. XXXX, XXX, XXX−XXX

Table 2. Crystallographic Data and Structural Refinement for 9-16

	9	10	11	12	13	14	15	16
formula	$C_{106}H_{74}GdMo_2N_{33}O_2$	$C_{106}H_{74}TbMo_2N_{33}O_2$	$C_{106}H_{74}DyMo_2N_{33}O_2$	$C_{106}H_{74}HoMo_2N_{33}O_2$	$C_{106}H_{74}ErMo_2N_{33}O_2$	$C_{106}H_{74}TmMo_2N_{33}O_2$	$C_{106}H_{74}YbMo_2N_{33}O_2$	$C_{106}H_{74}LuMo_2N_{33}O_2$
M_r	2191.11	2192.78	2196.36	2198.79	2201.12	2202.79	2206.9	2208.83
crystal system	monoclinic	monoclinic	monoclinic	monoclinic	monoclinic	monoclinic	monoclinic	monoclinic
space group	$C2/c$	$C2/c$	$C2/c$	$C2/c$	$C2/c$	$C2/c$	$C2/c$	$C2/c$
a (Å)	26.1990(11)	26.1707(11)	26.1547(17)	26.1460(17)	26.1241(14)	26.1124(12)	26.0740(10)	26.0579(13)
b (Å)	21.5420(9)	21.5304(12)	21.5207(14)	21.5421(13)	21.5106(12)	21.5072(10)	21.4857(8)	21.4663(10)
c (Å)	20.0728(8)	20.0608(9)	20.0557(13)	20.0800(12)	20.0585(11)	20.0633(9)	20.0437(7)	20.0369(10)
α (deg)	90.00	90.00	90.00	90.00	90.00	90.00	90.00	90.00
β (deg)	118.108(3)	118.056(3)	118.019(2)	117.990(3)	117.9330(10)	117.899(3)	117.872(3)	117.870(3)
γ (deg)	90.00	90.00	90.00	90.00	90.00	90.00	90.00	90.00
V (Å^3)	9992.6(7)	9975.3(8)	9965.6(11)	9986.9(11)	9958.6(9)	9958.0(8)	9926.2(6)	9908.0(8)
Z	4	4	4	4	4	4	4	4
ρ_c (g cm^{-3})	1.456	1.460	1.464	1.462	1.468	1.469	1.477	1.481
μ (mm^{-1})	0.972	1.018	1.059	1.101	1.152	1.200	1.252	1.307
total, unique	38205, 9774	38466, 9758	38081, 9755	37185, 9755	38341, 9733	37157, 9664	38099, 9710	37916, 9711
observed $[I > 2\sigma(I)]$	6553	6924	7180	7318	6843	7264	6916	6995
GOF on F^2	1.013	1.057	1.067	1.073	1.084	1.084	1.038	1.046
R_1, ωR_2 $[I > 2\sigma(I)]$	0.0547, 0.1389	0.0535, 0.1400	0.0542, 0.1369	0.0575, 0.1472	0.0530, 0.1295	0.0564, 0.1476	0.0534, 0.1303	0.0551, 0.1421
R_1, ωR_2 (all data)	0.0605, 0.1403	0.0579, 0.1410	0.0599, 0.1385	0.0618, 0.1486	0.0600, 0.1309	0.0624, 0.1494	0.0584, 0.1315	0.0616, 0.1435
CCDC number	1421801	1421802	1421803	1421804	1421805	1421806	1421807	1421808

DOI: 10.1021/acs.cgd.5b01782
Cryst. Growth Des. XXXX, XXX, XXX−XXX

and our continuing efforts into the study of magnetically coupled cyanide-bridged lanthanide materials, the present impetus is to further investigate the structures and magnetic properties of low-dimensional octacyanide-bridged lanthanide systems by combining the anionic $[Mo^{V}(CN)_8]^{3-}$ building block with highly anisotropic paramagnetic lanthanide ions Ln^{3+} (Ln = Gd−Lu) and the bidentate chelated ligand phen. A family of helical chains with the general formula $[Ln(phen)_2(H_2O)Mo(CN)_8]_2[(n\text{-}C_4H_9)_4N](NO_3)\cdot 2CH_3CN\cdot 4H_2O$ (Ln = Gd(**1**), Tb(**2**), Dy(**3**), Ho(**4**), Er(**5**), Tm(**6**), Yb(**7**), Lu(**8**)) were isolated, and these crystals underwent a remarkable resolvation-recrystallization process, affording a series of trinuclear clusters $(Hphen)_{2.5}[Ln_{0.5}(phen)(H_2O)][Mo(CN)_8]\cdot 1.5CH_3CN$ (Ln = Gd(**9**), Tb(**10**), Dy(**11**), Ho(**12**), Er(**13**), Tm(**14**), Yb(**15**), Lu(**16**)) upon prolonging the diffusion-reaction time. It should be worth mentioning that the octacyanometallate-based systems involving the phase conversion of structural dimensionalities are rarely explored. In fact, the structural dimensionalities did not changed, although humidity-, guest-, photo-, and thermal-, and pressure-induced phase conversions have been reported in related octacyanometallates.[35−40] Herein, we reported the syntheses, crystal structures, and magnetic studies of **1**−**16**.

EXPERIMENTAL SECTION

Materials and General Methods. All reagents were purchased from commercial sources and used without further purification. The $[HN(n\text{-}C_4H_9)_3]_3W(CN)_8$ precursor was prepared according to the published procedure.[41] Infrared (IR) spectra were recorded on a Nicolet FT 1703X spectrophotometer in the 4000−400 cm^{-1} region on KBr discs. Elemental analyses for C, H, and N were performed with a PerkinElmer 240C elemental analyzer. Powder X-ray diffraction (XRD) data were collected using a Shimadzu XRD-6000 diffractometer with Cu-K_α radiation. The detection of Ln and Mo atoms was performed with energy dispersive spectrometry (EDS, Oxford INCA). All magnetic measurements on microcrystalline samples were carried out on a Quantum Design MPMP-XL7 superconducting quantum interference device (SQUID) magnetometer. Corrections of measured susceptibilities were carried out considering both the sample holder as the background and the diamagnetism of the constituent atoms according to Pascal's tables.[42] Notably, the crystals of **1**−**8** are fragile and easily become powders upon removal from the mother liquid. Powder XRD analysis revealed the occurrence of structural transition (Figure S1) probably caused by the loss of solvents in the framework. Here, the magnetic properties of polycrystallines of **2** exposed in the air and covered by liquid paraffin were both investigated. Fortunately, the magnetic results showed that the magnetic curves of both samples exhibited an identical trend and features (Figure S2), which indicated that the magnetic properties of final polycrystallines have not changed despite the structural change upon being exposed in the air. So all magnetic measurements of **1**−**8** were carried out using the polycrystallines picked out from the mother liquid for convenience.

Syntheses. Single crystals of $[Ln(phen)_2(H_2O)Mo(CN)_8]_2[(n\text{-}C_4H_9)_4N](NO_3)\cdot 2CH_3CN\cdot 4H_2O$ (Ln = Gd(**1**), Tb(**2**), Dy(**3**), Ho(**4**), Er(**5**), Tm(**6**), Yb(**7**), Lu(**8**)) were prepared according to the reported method in the literature.[31] Yellow rod crystals of **1**−**8** were obtained after about 20 days, and these crystals gradually resolved and recrystallized with red block crystals of $(Hphen)_{2.5}[Ln_{0.5}(phen)(H_2O)][Mo(CN)_8]\cdot 1.5CH_3CN$ (Ln = Gd(**9**), Tb(**10**), Dy(**11**), Ho(**12**), Er(**13**), Tm(**14**), Yb(**15**), Lu(**16**)) after allowing the solution to stand for a further three months. The crystals of **1**−**8** are fragile and easily become powders upon removal from the mother liquid along with the structural change, while **9**−**16** exhibited high stability in the air. Powder XRD analysis of **9**−**16** indicated the high purities of polycrystalline samples (Figure S3). Atomic ratios (EDS results) of Mo/Ln for **9**−**16** are approximately equal to 2 for **9**: Mo/Gd = 1.91/1.00; for **10**: Mo/Tb = 1.92/1.00; for **11**: Mo/Dy = 1.90/1.00; for **12**: Mo/Ho = 1.87/1.00; for **13**: Mo/Er = 2.06/1.00; for **14**: Mo/Tm = 1.90/1.00; for **15**: Mo/Yb = 1.87/1.00; for **16**: Mo/Lu = 1.90/1.00. Anal. Calcd for $C_{106}H_{74}GdMo_2N_{33}O_2$ (**9**) (%): C, 58.11; H, 3.40; N, 21.10. Found: C, 57.99; H, 3.46; N, 21.17. Anal. Calcd for $C_{106}H_{74}TbMo_2N_{33}O_2$ (**10**) (%): C, 58.06; H, 3.40; N, 21.08. Found: C, 58.13; H, 3.37; N, 21.11. Anal. Calcd for $C_{106}H_{74}DyMo_2N_{33}O_2$ (**11**) (%): C, 57.97; H, 3.40; N, 21.05. Found: C, 58.00; H, 3.38; N, 21.01. Anal. Calcd for $C_{106}H_{74}HoMo_2N_{33}O_2$ (**12**) (%): C, 57.90; H, 3.39; N, 21.02. Found: C, 58.00; H, 3.35; N, 21.09. Anal. Calcd for $C_{106}H_{74}ErMo_2N_{33}O_2$ (**13**) (%): C, 57.84; H, 3.39; N, 21.00. Found: C, 57.79; H, 3.38; N, 21.07. Anal. Calcd for $C_{106}H_{74}TmMo_2N_{33}O_2$ (**14**) (%): C, 57.80; H, 3.39; N, 20.98. Found: C, 57.76; H, 3.42; N, 20.99. Anal. Calcd for $C_{106}H_{74}YbMo_2N_{33}O_2$ (**15**) (%): C, 57.69; H, 3.38; N, 20.94. Found: C, 57.65; H, 3.40; N, 21.01. Anal. Calcd for $C_{106}H_{74}LuMo_2N_{33}O_2$ (**16**) (%): C, 57.64; H, 3.38; N, 20.93. Found: C, 57.57; H, 3.40; N, 20.95. IR spectrum for **9**: $\nu_{C\equiv N}$ = 2109 cm^{-1}, 2135 cm^{-1}; for **10**: $\nu_{C\equiv N}$ = 2110 cm^{-1}, 2135 cm^{-1}; for **11**: $\nu_{C\equiv N}$ = 2110 cm^{-1}, 2135 cm^{-1}; for **12**: $\nu_{C\equiv N}$ = 2109 cm^{-1}, 2136 cm^{-1}; for **13**: $\nu_{C\equiv N}$ = 2111 cm^{-1}, 2136 cm^{-1}; for **14**: $\nu_{C\equiv N}$ = 2112 cm^{-1}, 2121 cm^{-1}; for **15**: $\nu_{C\equiv N}$ = 2114 cm^{-1}, 2136 cm^{-1}; for **16**: $\nu_{C\equiv N}$ = 2112 cm^{-1}, 2136 cm^{-1}.

X-ray Crystallographic Analysis. Single-crystal X-ray diffraction measurements of **1**−**16** were performed with a Bruker Apex II diffractometer using graphite monochromated molybdenum radiation [λ(Mo-K_α) = 0.71073 Å]. It should be noteworthy that the crystals of **1**−**8** were fragile and easily became powders after being exposed in the air. So single-crystal X-ray structural measurements of these crystals were performed by covering liquid paraffin on the single crystal. All diffraction data analysis and reduction were carried out within *SMART* and *SAINT*.[43] Correction for Lorentz, polarization, and absorption effects were performed within *SADABS*.[44] Structures were solved using Patterson method within *SHELXS-97* and refined using *SHELXL-97*.[45−47] All non-hydrogen atoms were refined with anisotropic thermal parameters. The hydrogen atoms of phen ligands, $[(n\text{-}C_4H_9)_4N]^+$ cations, and CH_3CN molecules were positioned with an idealized geometry and refined using a riding model. The hydrogen atoms of water molecules were located from difference Fourier maps and refined as riding model. CCDC numbers: 1421793−1421808 for **1**−**16**. This data can be obtained free of charge from the Cambridge Crystallographic Data Centre via www.ccdc.cam.ac.uk/data_request/cif. The crystallographic data and structural refinement for **1**−**16** are summarized in Tables 1 and 2.

RESULTS AND DISCUSSION

Crystal Structures. Single crystal XRD analysis indicated that the structures of **1**−**8** consist of 1D cyanide-bridged helical chains, isostructural to the $Ln^{III}Mo^{V}$ (Ln = Sm, Eu) complexes reported by our group.[31] Here the structure of **1** is described briefly. As shown in Figure 1, the asymmetric unit of **1** comprises one neutral $[Gd(phen)_2(H_2O)Mo(CN)_8]_2$ unit, one $[(n\text{-}C_4H_9)_4N]^+$ cation, one NO_3^- anion, and some disordered solvent molecules of water and acetonitrile. The eight-coordinated Mo and Gd centers are located in a slightly distorted square antiprism geometry. Then the $[Gd^{III}(phen)_2(H_2O)]^{3+}$ and $[Mo^{V}(CN)_8]^{3-}$ moieties are connected in an alternating manner by two *trans* cyanide groups, isolating the left- and right-handed helices running along the crystallographic 4_1 axis with a long pitch of about 16.78 Å (the Gd1···Gd1 distance) (Figure 2a). The Gd and Mo atoms in a pitch generate an eight-membered ring aperture viewed along the screw axis, in which nitrate anions and solvent molecules are located (Figure 2b). Adjacent helices are further packed through the relatively strong $\pi-\pi$ stacking interactions between aromatic rings of phen ligands, forming a 3D supramolecular network (Figure 2c). No obvious hydrogen-bonding interactions were observed in our system. To the best of our

DOI: 10.1021/acs.cgd.5b01782
Cryst. Growth Des. XXXX, XXX, XXX−XXX

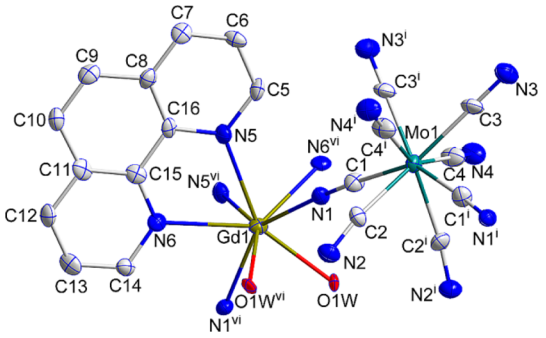

Figure 1. ORTEP diagram of **1** with thermal ellipsoids presented at the 30% probability level. All H atoms, $[(n\text{-}C_4H_9)_4N]^+$ cation, $[NO_3]^-$ anion, solvent CH_3CN and H_2O molecules have been omitted for clarity. Symmetry codes: (i) $y - 1/4, x + 1/4, -z + 1/4$; (vi) $-x + 1/2, y, -z$.

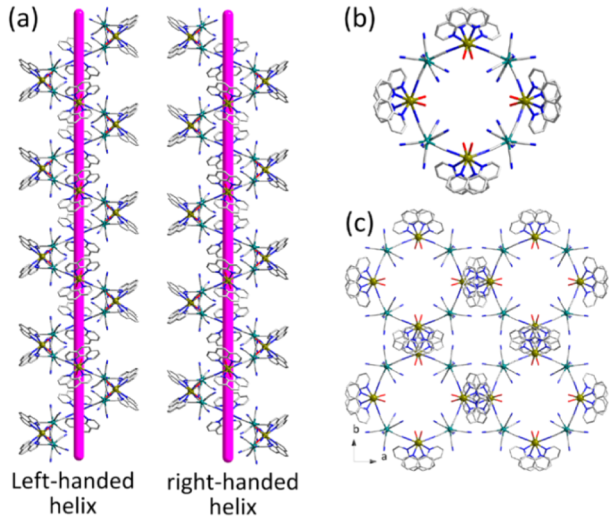

Figure 2. (a) The 1D left- and right-handed helices in the structure of **1**; (b) perspective view of the single-stranded helical chain along the 4_1 screw axis; (c) the 3D supramolecular network.

knowledge, there are limited examples of cyanide-bridged lanthanide complexes with helical structures to date.[29,31,48,49]

Interestingly, yellow rod crystals of **1**–**8** gradually transformed to red block crystals of **9**–**16** upon standing the solution for further three months, together with the obvious structural changes from helical chains to trinuclear molecules as well as the reduction of Mo atom from V to IV. Obviously, there is a resolvation–recrystallization process in both series, where the kinetically formed helical chains **1**–**8** are unstable thermodynamically and undergo transformation to the stable thermodynamically trinuclear products **9**–**16**. X-ray single crystal structural results revealed that **9**–**16** are also isomorphous, crystallizing in the monoclinic space group *C*2/*c*. Only the structure of **9** is described in detail, which contains the anionic $\{[Ln^{III}_{0.5}(phen)(H_2O)][Mo^{IV}(CN)_8]\}^{2.5-}$ trinuclear cluster with $(Hphen)^+$ charge-balance cations and uncoordinated molecules of acetonitrile.

The eight-coordinated Mo(IV) atom adopts a distorted square antiprismatic geometry, typical for octacyanomolybdates(IV).[50−53] Two *trans* cyanide ligands in $[Mo^{IV}(CN)_8]^{4-}$ acting as linear two-connectors bridge to two adjacent $[Ln^{III}_{0.5}(phen)(H_2O)]^{1.5+}$ moieties, while the remaining six ones are terminal. The average Mo1–C and C–N bond

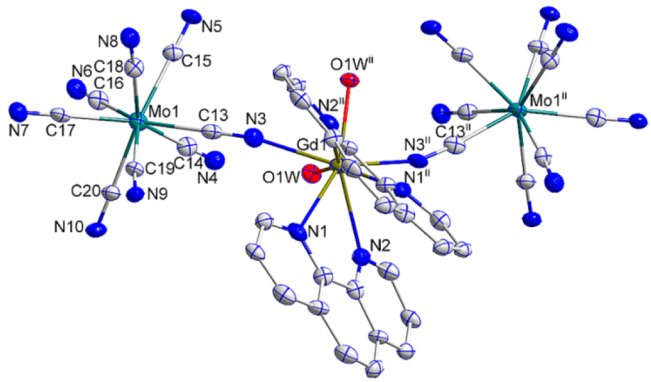

Figure 3. Trinuclear cluster structure of **9** with thermal ellipsoids presented at the 30% probability level. All H atoms, $(Hphen)^+$ cations, and CH_3CN molecules have been omitted for clarity. Symmetry code: (ii) $x, y, -z + 3/2$.

distances are about 2.163 and 1.158 Å, respectively, and all Mo1-CN units exhibit almost linear with the maximum deviation from linearity of 5.5°. The Gd(III) atom is eight-coordinated and lies in a slightly distorted square antiprismatic environment with two cyanide-nitrogen atoms, four nitrogen atoms from two phen ligands and two oxygen atoms from coordinated water molecules. The average Gd1–N and Gd1–O bond lengths are approximately 2.520 and 2.368 Å, respectively. The Gd1–NC bonds are significantly bent with the angle of 161.5(4)°, opposition to the linear Mo1-CN units. The geometrical data of the Gd1–N_{phen} and Gd1–O bonds are identical to those observed in related cyanide-bridged lanthanide-phen complexes.[31,54−56]

As a result, the $[Mo^{IV}(CN)_8]^{4-}$ and $[Ln^{III}_{0.5}(phen)(H_2O)]^{1.5+}$ units are linked in an alternating fashion through *trans* cyanide groups to generate an anionic trinuclear cluster $\{[Ln^{III}_{0.5}(phen)(H_2O)][Mo(CN)_8]\}^{2.5-}$ cocrystallized with charge-balance $(Hphen)^+$ cations. The similar trinuclear clusters have also been found in hexa-, hepta- and octacyanometallate-based bimetallic complexes.[57−64] The intracluster Mo···Gd and Mo···Mo distances are about 5.628 and 10.316 Å, respectively. The neighboring trinuclear units are separated through well-defined hydrogen-bonding interactions and π–π stacking interactions of aromatic rings of phen ligands, isolating the formation of a 3D supramolecular network (Figure 4). The intermolecular Gd···Gd, Mo···Gd, and Mo···Mo distances are about 11.831, 10.754, and 10.193 Å, respectively.

After careful comparison, there are some similarities between the crystal structures of the two series. The Ln atoms in **1**–**16** show the same distorted square antiprismatic geometry, being eight-coordinated to two bridging cyanide groups, four terminal cyanide groups and two water molecules. With the experimental error, there are no significant differences in the bond lengths of Ln–N, Ln–O, and N–C (Table S1, Figure S4). Also, the metric parameters of bond lengths and angles around the Mo centers of both series are almost identical to each other. To some extent, the resulting trinuclear clusters (**9**–**16**) seem to be a fragment of the corresponding 1D helices (**1**–**8**). The major differences between the structures of both series are as follows: (i) there are two bridging cyanide groups in the $[Mo(CN)_8]$ unit for **1**–**8**, while only one was found for **9**–**16**. (ii) the Ln-NC bonds in **1**–**8** are nearly linear, whereas the bonds are significantly bent for **9**–**16**. (iii) the Ln atom and the coordinated phen ligand are almost in the same plane for **1**–**8**, while the obvious deviation was observed in **9**–**16**. These

DOI: 10.1021/acs.cgd.5b01782
Cryst. Growth Des. XXXX, XXX, XXX–XXX

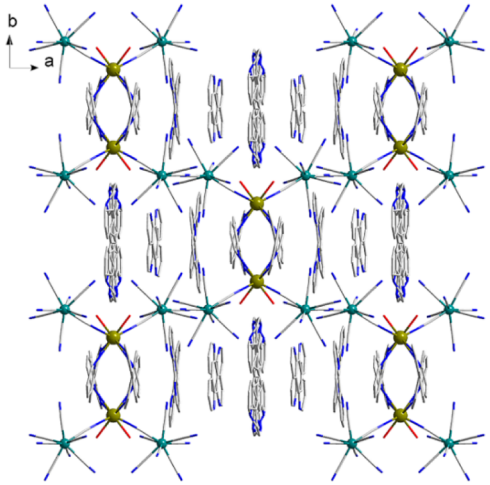

Figure 4. 3D supramolecular network of **9**.

differences perhaps give rise to the formation of 1D helices (**1**−**8**) and discrete clusters (**9**−**16**) together with the various stacking networks.

Magnetic Properties. The dc temperature-dependent molar magnetic susceptibilities of **1**−**16** were measured under 100 Oe. As shown in Figure 5a,c, the room temperature $\chi_M T$ values of **1**−**16** are overall within the range expected for the corresponding $Ln^{III}Mo^{III}$/$Ln^{III}Mo^{III}_2$ units (Table 3). For **1**−**7**, the room temperature $\chi_M T$ values are higher than the theoretical ones, while **9**−**16** show the opposite trend except for **14**. As the temperature decreases, the $\chi_M T$ values of these series of complexes mainly exhibit the decrease feature until reaching the minimum values at 1.8 K, respectively. These magnetic behaviors are typical of properties shown by these 5d-4f systems, in which the spin−orbit coupling, the thermal depopulation of the Stark sublevels as well as the exchange interaction might be presented together.[65−68] As far as we known, there are no suitable models to be used for simulating the magnetic data of **1**−**16**. However, the $Gd^{III}Mo^{III}$/$Gd^{III}Mo^{III}_2$ systems without single ion anisotropy could provide us some information for understanding the magnetic nature of these complexes. From the $\chi_M T$ vs T curves of **1** and **9**, it is found that the intramolecular magnetic couplings of both complexes are very weak (the curves keep almost constant upon cooling). Therefore, the exchange interactions in these isostructural systems should be also very weak, and the magnetic thermal behaviors are actually dominated by the single ion properties of 4f ions.[69] The coordination environments around 4f ions often affect such single ion properties especially when the magnetic anisotropy related to slow magnetic relaxations is concerned. To verify the single ion properties of these complexes, the dc field-dependent magnetizations were measured at 1.8 K (Figure 5b,d). As the applied fields increase, the magnetization values increase accordingly, showing the characteristic behaviors expected for the Ln^{III}-based complexes. Except for **2**, the magnetization values of **3**−**16** have not reached the theoretical saturated ones even at 70 kOe (Table 3), revealing the effect induced by single ion magnetic anisotropy and/or the population of low-lying excited states.[70−74]

To study the magnetic relaxation dynamics of these complexes, ac susceptibility measurements were conducted. The results indicate that **11** and **13** show field-induced slow magnetic relaxations,[75,76] as shown in Figure 6. No further dynamics investigations can be done due to the lack of maximum values above 1.8 K. The slow magnetic relaxations of **11** and **13** are obviously induced by the magnetic anisotropy

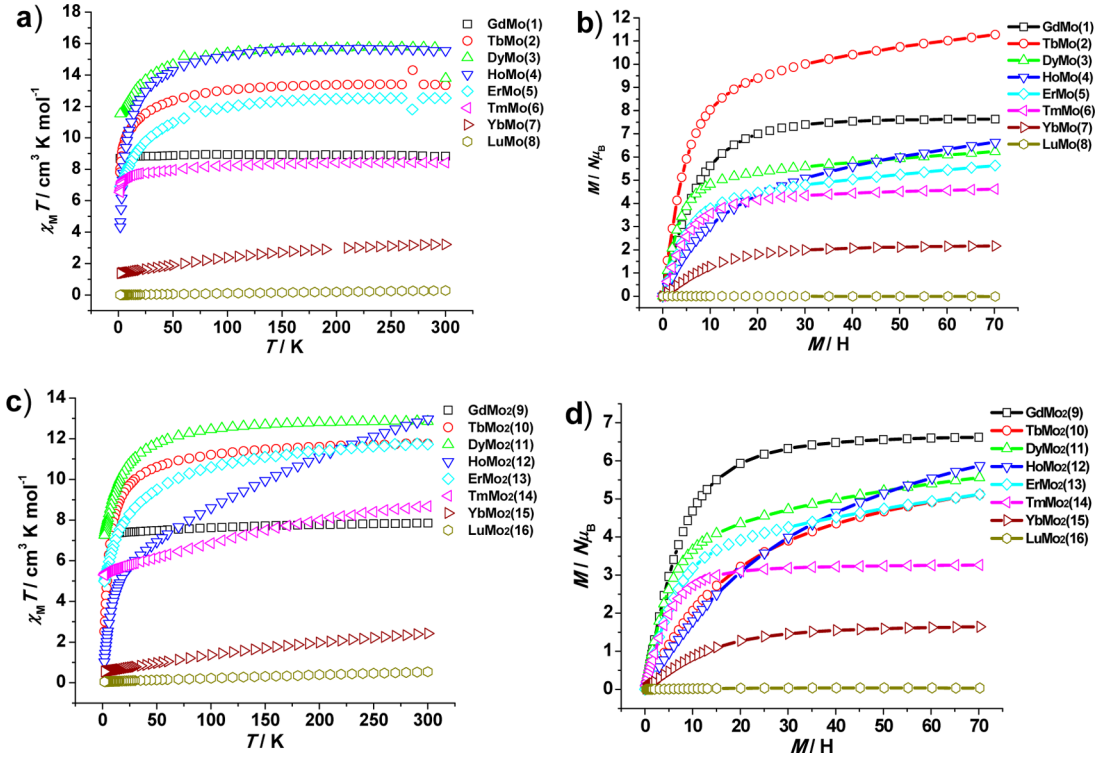

Figure 5. Temperature dependence of $\chi_M T$ for **1**−**8** (a) and **9**−**16** (c) measured at 100 Oe; Field dependence of the magnetization for **1**−**8** (b) and **9**−**16** (d) measured at 1.8 K.

DOI: 10.1021/acs.cgd.5b01782
Cryst. Growth Des. XXXX, XXX, XXX−XXX

Table 3. Comparison of $\chi_M T$ and Magnetization Values (Experimental and Theoretical) of 1−16

complex	1	2	3	4	5	6	7	8
experimental room-temperature $\chi_M T$ value	8.84	13.34	15.75	15.56	12.54	8.42	3.20	0.28
Ttheoretical room-temperature $\chi_M T$ value	8.25	12.19	14.54	14.44	11.85	7.52	2.94	0.37
experimental magnetization value at 70 kOe	7.63	11.28	6.24	6.63	5.63	4.61	2.16	−0.03
theoretical saturated magnetization value	8	10	11	11	10	8	5	1
complex	**9**	**10**	**11**	**12**	**13**	**14**	**15**	**16**
experimental room-temperature $\chi_M T$ value	7.85	11.76	12.85	12.97	11.72	8.68	2.42	0.54
theoretical room-temperature $\chi_M T$ value	8.62	12.56	14.91	14.81	12.22	7.89	3.31	0.74
experimental magnetization value at 70 kOe	6.61	5.11	5.56	5.87	5.11	3.26	1.64	0.03
theoretical saturated magnetization value	9	11	12	12	11	9	6	2

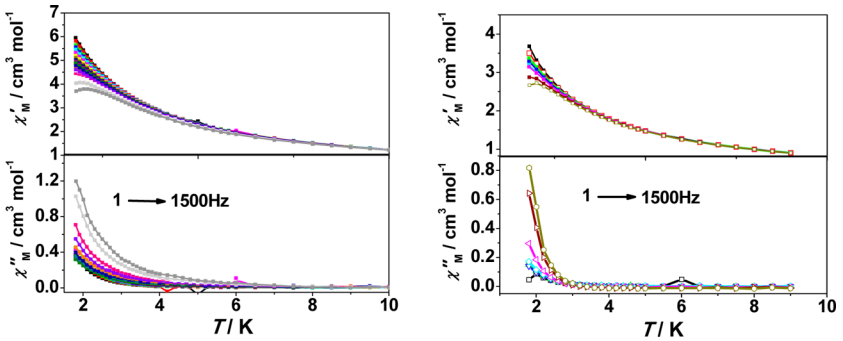

Figure 6. Temperature dependence of the in-phase (χ'_M) out-of-phase (χ''_M) ac susceptibilities of **11** (left) and **13** (right) in 600 Oe dc field and 3 Oe ac field (solid lines are guides for the eyes).

brought by Dy^{III} and Er^{III}. However, complexes **3** and **5** which also contain Dy^{III} or Er^{III} show no slow magnetic relaxations. Considering that the local geometries around lanthanide ions in these series of complexes are almost identical (as revealed by the structural analysis), the vanishing of the slow magnetic relaxations of **3** and **5** might be caused by the weak magnetic interactions between the subunit of trinuclear LnM_2 (M = W, Mo) clusters in the chains. Indeed, the trinuclear LnM_2 (M = W, Mo) clusters are only well isolated to each other in the series of complexes **9**−**16**. Nevertheless, it is also difficult to explain the lack of any slow magnetic relaxation of **10**, which has the same structural parameters to **11** and **13**, and also contains the magnetic anisotropic spin center (Tb^{III} ions). Consequently, the peculiar coordination geometry around the Dy^{III} and Er^{III} centers does enhance the magnetic anisotropy and produces the energy barrier for reversing the magnetization, but the intercluster magnetic interactions produce a negative effect on the slow magnetic relaxtions.[77] Besides, the relaxation process is also seriously interfered by the quantum tunneling effect, which can significantly speed up the relaxation process, leading to the field-induced slow magnetic relaxations.[78]

CONCLUSIONS

To summarize, the foregoing results in this contribution demonstrate a facile strategy to generate low-dimensional octacyanide-bridged lanthanide systems with the incorporation of paramagnetic $[Mo^{V}(CN)_8]^{3-}$ and lanthanide ions in the presence of aromatic chelated ligands. More importantly, a series of isostructural trinuclear clusters were gradually generated from the crystals of helical chains by prolonging the diffusion reaction time, in which an unprecedented change with structural dimensionalities in octacyanide-bridged systems was involved. Note that this resolvation−recrystallization process opens up the perspectives and potential applications in molecular devices such as switches and sensors, although the fascinating slow magnetic relaxations were only observed in two complexes. Work currently under progress in our lab is devoted to the exploration of other chains or clusters, as well as the elucidation of drastic structural conversions and appealing magnetic behaviors. Also, we focus on the discovery of the close structure-magnetism relationships of low-dimensional octacyanometallate-based systems in the near future.

ASSOCIATED CONTENT

Supporting Information

The Supporting Information is available free of charge on the ACS Publications website at DOI: 10.1021/acs.cgd.5b01782.

Figures S1 and S3: Powder XRD patterns; Figure S2: (a) Temperature dependence of $\chi_M T$, field dependence of the magnetization at different temperatures, and temperature dependence of ac susceptibilities; Table S1: Detailed structural parameters around the Gd and Mo centers in **1** and **9**; Figure S4: The local geometries around the Gd ion in **1** and **9** (PDF)

Accession Codes

CCDC 1421793−1421808 contains the supplementary crystallographic data for this paper. These data can be obtained free of charge via www.ccdc.cam.ac.uk/data_request/cif, or by emailing data_request@ccdc.cam.ac.uk, or by contacting The Cambridge Crystallographic Data Centre, 12, Union Road, Cambridge CB2 1EZ, UK; fax: +44 1223 336033.

AUTHOR INFORMATION

Corresponding Authors

*(A.H.Y.) Tel: +86 511 85639001. Fax: +86 511 85635850. E-mail: aihua.yuan@just.edu.cn.
*(Y.S.) yousong@nju.edu.cn.

DOI: 10.1021/acs.cgd.5b01782
Cryst. Growth Des. XXXX, XXX, XXX−XXX

Notes

The authors declare no competing financial interest.

■ ACKNOWLEDGMENTS

The authors are grateful for financial support from the National Natural Science Foundation (51102119, 51272095), Natural Science Foundation of Jiangsu Province (BK20151328), Qing Lan Project of Jiangsu Province, the project of the Priority Academic Program Development of Jiangsu Higher Education Institutions, China Postdoctoral Science Foundation (2014M561578), and Jiangsu Planned Projects for Postdoctoral Research Funds (1401109C).

■ REFERENCES

(1) Miller, J. S.; Gatteschi, D. *Chem. Soc. Rev.* **2011**, *40*, 3065−3066.
(2) Hatlevik, Ø.; Buschmann, W. E.; Zhang, J.; Manson, J. L.; Miller, J. S. *Adv. Mater.* **1999**, *11*, 914−918.
(3) Holmes, S. M.; Girolami, G. S. *J. Am. Chem. Soc.* **1999**, *121*, 5593−5594.
(4) Ferlay, S.; Mallah, T.; Ouahès, R.; Veillet, P.; Verdaguer, M. *Nature* **1995**, *378*, 701−703.
(5) Pardo, E.; Train, C.; Liu, H. B.; Chamoreau, L. M.; Dkhil, B.; Boubekeur, K.; Lloret, F.; Nakatani, K.; Tokoro, H.; Ohkoshi, S.; Verdaguer, M. *Angew. Chem., Int. Ed.* **2012**, *51*, 8356−8360.
(6) Ohkoshi, S.; Tokoro, H.; Matsuda, T.; Takahashi, H.; Irie, H.; Hashimoto, K. *Angew. Chem., Int. Ed.* **2007**, *46*, 3238−3241.
(7) Milon, J.; Daniel, M. C.; Kaiba, A.; Guionneau, P.; Brandès, S.; Sutter, J. P. *J. Am. Chem. Soc.* **2007**, *129*, 13872−13878.
(8) Yanai, N.; Kaneko, W.; Yoneda, K.; Ohba, M.; Kitagawa, S. *J. Am. Chem. Soc.* **2007**, *129*, 3496−3497.
(9) Ohkoshi, S.; Arai, K.; Sato, Y.; Hashimoto, K. *Nat. Mater.* **2004**, *3*, 857−861.
(10) Yang, F. L.; Yuan, A. H.; Zhou, H.; Zhou, H. B.; Yang, D.; Song, Y.; Li, Y. Z. *Cryst. Growth Des.* **2015**, *15*, 176−184.
(11) Koumousi, E. S.; Jeon, I. R.; Gao, Q.; Dechambenoit, P.; Woodruff, D. N.; Merzeau, P.; Buisson, L.; Jia, X. L.; Li, D. F.; Volatron, F.; Mathonière, C.; Clérac, R. *J. Am. Chem. Soc.* **2014**, *136*, 15461−15464.
(12) Ohkoshi, S.; Tokoro, H. *Acc. Chem. Res.* **2012**, *45*, 1749−1758.
(13) Ohkoshi, S.; Imoto, K.; Tsunobuchi, Y.; Takano, S.; Tokoro, H. *Nat. Chem.* **2011**, *3*, 564−569.
(14) Pajerowski, D. M.; Andrus, M. J.; Gardner, J. E.; Knowles, E. S.; Meisel, M. W.; Talham, D. R. *J. Am. Chem. Soc.* **2010**, *132*, 4058−4059.
(15) Yoo, J. W.; Edelstein, R. S.; Lincoln, D. W.; Raju, N. P.; Epstein, A. J. *Phys. Rev. Lett.* 2007, *99*, No. 157205.
(16) Lim, J. H.; Yoo, H. S.; Kim, J., II.; Yoon, J. H.; Yang, N.; Koh, E. K.; Park, J. G.; Hong, C. S. *Eur. J. Inorg. Chem.* **2008**, *2008*, 3428−3431.
(17) Lim, J. H.; Yoo, H. S.; Yoon, J. H.; Koh, E. K.; Kim, H. C.; Hong, C. S. *Polyhedron* **2008**, *27*, 299−303.
(18) Freedman, D. E.; Bennett, M. V.; Long, J. R. *Dalton Trans.* **2006**, 2829−2834.
(19) Lim, J. H.; Yoon, J. H.; Kim, H. C.; Hong, C. S. *Angew. Chem., Int. Ed.* **2006**, *45*, 7424−7426.
(20) Ruiz, E.; Rajaraman, G.; Alvarez, S.; Gillon, B.; Stride, J.; Clérac, R.; Larionova, J.; Decurtins, S. *Angew. Chem., Int. Ed.* **2005**, *44*, 2711−2715.
(21) Song, Y.; Zhang, P.; Ren, X. M.; Shen, X. F.; Li, Y. Z.; You, X. Z. J. *J. Am. Chem. Soc.* **2005**, *127*, 3708−3709.
(22) Larionova, J.; Gross, M.; Pilkington, M.; Andres, H.; Stoeckli-Evans, H.; Güdel, H. U.; Decurtins, S. *Angew. Chem., Int. Ed.* **2000**, *39*, 1605−1609.
(23) Zhong, Z. J.; Seino, H.; Mizobe, Y.; Hidai, M.; Fujishima, A.; Ohkoshi, S.; Hashimoto, K. *J. Am. Chem. Soc.* **2000**, *122*, 2952−2953.
(24) Zhang, Y. Z.; Zhao, H. H.; Funck, E.; Dunbar, K. R. *Angew. Chem., Int. Ed.* **2015**, *54*, 5583−5587.
(25) Yoon, J. H.; Lee, J. W.; Ryu, D. W.; Choi, S. Y.; Yoon, S. W.; Suh, B. J.; Koh, E. K.; Kim, H. C.; Hong, C. S. *Inorg. Chem.* **2011**, *50*, 11306−11308.
(26) Yoon, J. H.; Ryu, D. W.; Choi, S. Y.; Kim, H. C.; Koh, E. K.; Tao, J.; Hong, C. S. *Chem. Commun.* **2011**, *47*, 10416−10418.
(27) Venkatakrishnan, T. S.; Sahoo, S.; Bréfuel, N.; Duhayon, C.; Paulsen, C.; Barra, A. L.; Ramasesha, S.; Sutter, J. P. *J. Am. Chem. Soc.* **2010**, *132*, 6047−6056.
(28) Visinescu, D.; Madalan, A. M.; Andruh, M.; Duhayon, C.; Sutter, J. P.; Ungur, L.; Van den Heuvel, W.; Chibotaru, L. F. *Chem. - Eur. J.* **2009**, *15*, 11808−11814.
(29) Yu, D. Y.; Li, L.; Zhou, H.; Yuan, A. H.; Li, Y. Z. *Eur. J. Inorg. Chem.* **2012**, *2012*, 3394−3397.
(30) Yang, X. Z.; Zhou, H.; Qian, S. Y.; Yuan, A. H.; Zhou, H. B.; Song, Y. *Inorg. Chem. Commun.* **2012**, *24*, 40−42.
(31) Qian, S. Y.; Zhou, H.; Yuan, A. H.; Song, Y. *Cryst. Growth Des.* **2011**, *11*, 5676−5681.
(32) Yuan, A. H.; Qian, S. Y.; Liu, W. Y.; Zhou, H.; Song, Y. *Dalton Trans.* **2011**, *40*, 5302−5306.
(33) Ferbinteanu, M.; Cimpoesu, F.; Tanase, S. *Metal-Organic Frameworks with d-f Cyanide Bridges: Structural Diversity, Bonding Regime, and Magnetism. Lanthanide Metal-Organic Frameworks*; Cheng, P., Ed.; Springer-Verlag Berlin: Berlin. 2015; pp *163*, 185−229.
(34) Andruh, M.; Costes, J. P.; Diaz, C.; Gao, S. *Inorg. Chem.* **2009**, *48*, 3342−3359.
(35) Ozaki, N.; Tokoro, H.; Miyamoto, Y.; Ohkoshi, S. *New J. Chem.* **2014**, *38*, 1950−1954.
(36) Ozaki, N.; Tokoro, H.; Hamada, Y.; Namai, A.; Matsuda, T.; Kaneko, S.; Ohkoshi, S. *Adv. Funct. Mater.* **2012**, *22*, 2089−2093.
(37) Pinkowicz, D.; Kurpiewska, K.; Lewiński, K.; Balanda, M.; Mihalik, M.; Zentková, M.; Sieklucka, B. *CrystEngComm* **2012**, *14*, 5224−5229.
(38) Podgajny, R.; Chorąży, S.; Nitek, W.; Budziak, A.; Rams, M.; Gómez-García, C. J.; Oszajca, M.; Łasocha, W.; Sieklucka, B. *Cryst. Growth Des.* **2011**, *11*, 3866−3876.
(39) Nowicka, B.; Bałanda, M.; Gaweł, B.; Ćwiak, G.; Budziak, A.; Łasocha, W.; Sieklucka, B. *Dalton Trans.* **2011**, *40*, 3067−3073.
(40) Gheorghe, R.; Kalisz, M.; Clérac, R.; Mathonière, C.; Herson, P.; Li, Y. L.; Seuleiman, M.; Lescouëzec, R.; Lloret, F.; Julve, M. *Inorg. Chem.* **2010**, *49*, 11045−11056.
(41) Bok, L. D. C.; Leipoldt, J. G.; Basson, S. S. *Z. Anorg. Allg. Chem.* **1975**, *415*, 81−83.
(42) Kahn, O. *Molecular Magnetism*; VCH Publisher: New York, 1993.
(43) Bruker; *SMART, SAINT and XPREP: Area Detector Control and Data Integration and Reduction Software*; Bruker Analytical X-ray Instruments Inc.: Madison, Wisconsin, USA, 1995.
(44) Sheldrick, G. M. *SADABS: Empirical Absorption and Correction Software*; University of Göttingen: Göttingen, Germany, 1996.
(45) Sheldrick, G. M. *SHELXS-97. Program for X-ray Crystal Structure Determination*; Göttingen University: Göttingen, Germany, 1997.
(46) Sheldrick, G. M. *SHELXL-97. Program for X-ray Crystal Structure Determination*; Göttingen University: Göttingen, Germany, 1997.
(47) Sheldrick, G. M. A short history of SHELX. *Acta Crystallogr., Sect. A: Found. Crystallogr.* **2008**, *64*, 112−122.
(48) Chorazy, S.; Nakabayashi, K.; Arczynski, M.; Pełka, R.; Ohkoshi, S.; Sieklucka, B. *Chem.−Eur. J.* **2014**, *20*, 7144−7159.
(49) Chorazy, S.; Nakabayashi, K.; Ozaki, N.; Pełka, R.; Fic, T.; Mlynarski, J.; Sieklucka, B.; Ohkoshi, S. *RSC Adv.* **2013**, *3*, 1065−1068.
(50) Qian, S. Y.; Zhou, H.; Liu, W. Y.; Yuan, A. H. *J. Coord. Chem.* **2010**, *63*, 3914−3922.
(51) Yuan, A. H.; Liu, W. Y.; Zhou, H.; Qian, S. Y. *J. Coord. Chem.* **2009**, *62*, 3592−3598.
(52) Zhou, H.; Chen, Y. Y.; Yuan, A. H.; Shen, X. P. *Inorg. Chem. Commun.* **2008**, *11*, 363−366.
(53) Yuan, A. H.; Zhou, H.; Chen, Y. Y.; Shen, X. P. *J. Mol. Struct.* **2007**, *826*, 165−169.
(54) Huang, Y. F.; Wei, H. H.; Katada, M. *J. Coord. Chem.* **2008**, *61*, 2683−2689.

DOI: 10.1021/acs.cgd.5b01782
Cryst. Growth Des. XXXX, XXX, XXX−XXX

(55) Koner, R.; Drew, M. G. B.; Figuerola, A.; Diaz, C.; Mohanta, S. *Inorg. Chim. Acta* **2005**, *358*, 3041−3047.
(56) Gao, S.; Ma, B. Q.; Sun, H. L.; Li, J. R. *J. Solid State Chem.* **2003**, *171*, 201−207.
(57) Liu, T.; Dong, D. P.; Kanegawa, S.; Kang, S.; Sato, O.; Shiota, Y.; Yoshizawa, K.; Hayami, S.; Wu, S.; He, C.; Duan, C. Y. *Angew. Chem., Int. Ed.* **2012**, *51*, 4367−4370.
(58) Shen, X. P.; Zhang, Q.; Zhou, H. B.; Zhou, H.; Yuan, A. H. *New J. Chem.* **2012**, *36*, 1180−1186.
(59) Qian, K.; Huang, X. C.; Zhou, C.; You, X. Z.; Wang, X. Y.; Dunbar, K. R. *J. Am. Chem. Soc.* **2013**, *135*, 13302−13305.
(60) Yang, C.; Wang, Q. L.; Su, C. Y.; Hu, L. N.; Li, L. C.; Liao, D. Z. *Inorg. Chem. Commun.* **2014**, *40*, 26−30.
(61) Xu, H. T.; Sato, O.; Li, Z. H.; Ma, J. P. *Inorg. Chem. Commun.* **2012**, *15*, 311−313.
(62) Zhang, W.; Sun, H. L.; Sato, O. *Dalton Trans.* **2011**, *40*, 2735−2743.
(63) Wang, Z. X.; Wei, H.; Li, Y. Z.; Guo, J. S.; Song, Y. *J. Mol. Struct.* **2008**, *875*, 198−204.
(64) Visinescu, D.; Desplanches, C.; Imaz, I.; Bahers, V.; Pradhan, R.; Villamena, F. A.; Guionneau, P.; Sutter, J. P. *J. Am. Chem. Soc.* **2006**, *128*, 10202−10212.
(65) Zhao, L.; Wu, J. F.; Ke, H. S.; Tang, J. K. *Inorg. Chem.* **2014**, *53*, 3519−3525.
(66) Jana, A.; Majumder, S.; Carrella, L.; Nayak, M.; Weyhermueller, T.; Dutta, S.; Schollmeyer, D.; Rentschler, E.; Koner, R.; Mohanta, S. *Inorg. Chem.* **2010**, *49*, 9012−9025.
(67) Estrader, M.; Ribas, J.; Tangoulis, V.; Solans, X.; Font-Bardia, M.; Maestro, M.; Diaz, C. *Inorg. Chem.* **2006**, *45*, 8239−8250.
(68) Gheorghe, R.; Cucos, P.; Andruh, M.; Costes, J. P.; Donnadieu, B.; Shova, S. *Chem. - Eur. J.* **2006**, *12*, 187−203.
(69) Feltham, H. L. C.; Brooker, S. *Coord. Chem. Rev.* **2014**, *276*, 1−33.
(70) Chorazy, S.; Arczynski, M.; Nakabayashi, K.; Sieklucka, B.; Ohkoshi, S. *Inorg. Chem.* **2015**, *54*, 4724−4736.
(71) Zhu, J.; Wang, C. Z.; Luan, F.; Liu, T. Q.; Yan, P. F.; Li, G. M. *Inorg. Chem.* **2014**, *53*, 8895−8901.
(72) Zhou, H.; Diao, G. W.; Qian, S. Y.; Yang, X. Z.; Yuan, A. H.; Song, Y.; Li, Y. Z. *Dalton Trans.* **2012**, *41*, 10690−10697.
(73) Zhou, H.; Yuan, A. H.; Qian, S. Y.; Song, Y.; Diao, G. W. *Inorg. Chem.* **2010**, *49*, 5971−5976.
(74) Sessoli, R.; Powell, A. K. *Coord. Chem. Rev.* **2009**, *253*, 2328−2341.
(75) Nedelko, N.; Kornowicz, A.; Justyniak, I.; Aleshkevych, P.; Prochowicz, D.; Krupiński, P.; Dorosh, O.; Slawska-Waniewska, A.; Lewiński, J. *Inorg. Chem.* **2014**, *53*, 12870−12876.
(76) Fortea-Pérez, F. R.; Vallejo, J.; Julve, M.; Lloret, F.; De Munno, G.; Armentano, D.; Pardo, E. *Inorg. Chem.* **2013**, *52*, 4777−4779.
(77) Bridonneau, N.; Gontard, G.; Marvaud, V. *Dalton Trans.* **2015**, *44*, 5170−5178.
(78) Gunther, L.; Barbara, B., Eds. *Quantum Tunnelling of Magnetization: QTM '94*; NATO ASI Series E, Applied Sciences; Kluwer Academic Publishers: Boston, MA, 1995; Vol. *301*.

DOI: 10.1021/acs.cgd.5b01782
Cryst. Growth Des. XXXX, XXX, XXX−XXX